PERFORMANCE TRADE-OFFS FOR MBG CELLS USING DIFFERENT BANDGAP PAIRS [1]

P.A. Iles, C.L. Chu and L. Kilmer
TECSTAR/ASD, City of Industry, CA 91745-1002
M.L. Timmons, P. Sharps
Research Triangle Institute, R.T. Park, NC 27709

BACKGROUND

Present $GaInP_2$/GaAs cells grown on Ge (or GaAs) substrates have demonstrated high efficiency. However, the individual bandgaps (1.85 eV, 1.42 eV respectively) are not the optimum match to convert the AM0 spectrum efficiently, although by reducing the thickness of the $GaInP_2$ cell, good efficiencies have been achieved.

Within the III-V alloys, modeling shows that several dual junction cells, comprising different bandgap pairs, could give higher efficiency.

This paper outlines the modeling used, the bandgap pairs selected, and projections for the AM0 efficiency assuming that the effects of lattice mismatch associated with the bandgap pairs can be reduced. We also present preliminary data on I-V performance for the selected top and bottom cells and for some full cascade cells. We have included some characterization results to check the bandgaps and lattice strain, to check how closely the fabricated cells conform to the model.

<u>Note</u>
In order to use continuous access to an MOCVD reactor dedicated to this project, we decided to scan across the bandgap (and lattice constant) range, rather than use systematically increasing lattice mismatch of selected bandgap pairs, to check the main problem areas in characterization and cell performance. We also prepared one set of Ge substrates with a thin GaAs seeding layer to cover all the MOCVD runs; in retrospect, these substrates may have reduced the quality of the ternary compounds grown on these substrates.

MODELING

<u>Estimates for Optimum Bandgap Combinations</u>
To estimate the optimum bandgap combinations we used the following format, based on the bandgap versus lattice constant plot for III-V alloys, shown in Figure 1.

1) We varied the y value in $Ga_yIn_{1-y}As$ from 1.0 (GaAs) down to 0.6, using approximate Δy increments of 0.05.
2) For these different y-values, we computed the $Ga_yIn_{1-y}As$ energy gap from the expression $Eg=0.36 + 1.064y$ and the lattice constant a_o from Vegard's Law, where a_o scales linearly with composition, between the a_o-value for GaAs = 5.6532A°, and the a_o-value
3) For these selected y-values, using Vegard's Law, we estimated the x values in $Ga_xIn_{1-x}P$ which gives the same a_0 value as the GaInAs alloys.
4) Using the expression $Eg = 1.351 + 0.643x + 0.78x^2$, we calculated the Eg-values corresponding to the various x-values in $Ga_xIn_{1-x}P$.

The results of these computations are given in Table 1, where bandgap pairs A through I are listed, with their corresponding x and y values, along with the lattice-mismatch with respect to Ge or GaAs.

Table 1 also shows a column of theoretical AM0 efficiency values as a function of bandgap pair values, taken from Fan (1) or Wanlass (2). For reference in the table, we have included the bandgap pair J, the InP/InGaAs combination.

Figure 2 shows the theoretical AM0 efficiency for the selected Eg-pairs where the abscissa is the lattice mismatch wrt Ge (Curve A). The points plotted do not give a smooth curve because the Eg-pairs were selected from compounds which were on the tie-lines for the ternary compounds GaInAs and GaInP. The figure does not include the degrading effects of lattice-mismatch. The determination of the trade-off between practical efficiency and lattice-mismatch effects is the purpose of this study.

In Figure 2, curve B shows estimates of how practical efficiency values, again not corrected for lattice-mismatch, will vary for the cells with different Eg-pairs. We have used the practical efficiency $\approx 25.5\%$ achieved for cells comprising $Ga_{0.5}In_{0.5}P$ and GaAs, grown monolithically, to draw the curve B.

Also in Figure 2 are two "estimated" curves, showing the trends in practical efficiency, when lattice-grading is used (curve C), or when no grading is used (curve D). This study is intended to provide data to determine practical curves like C and D.

EXPERIMENTAL DATA

Cell Growth
Three sets of cells were MOCVD-grown at RTI, mostly on GaAs/Ge substrates, namely:
a) $Ga_xIn_{1-x}As$ structures, where the lattice-grading structures were as shown in Figure 3.
b) $Ga_yIn_{1-y}P$ cells grown on the buffer (lattice-grading) layers of $Ga_zIn_{1-z}As$, where the x values were selected from the modeling, to give lattice-match to the corresponding z-values. Figure 4 shows the layer scheme,
c) Tandem cells - $Ga_yI_{1-y}P$ cells grown on $Ga_xIn_{1-x}As$ cells, using buffer layers of $Ga_zIn_{1-z}As$, where the x and y values correspond to theoretical lattice match composition. Figure 5 shows the layer scheme.

In previous tests, RTI established that an effective tunnel junction could be formed in lattice-mismatched GaInAs over the range of z-values used in this study.

Cell Fabrication
RTI had grown a GaInAs cap layer with the same x-value as the selected composition, on all the cell structures. We decided to use a "universal" cap-etch solution and the same front side metallization for all the structures, and we did not experience any problems resulting from this choice.

Some of the wafers (not always those involving the greatest lattice-mismatch) were bowed, and to reduce the chance of breakage the processing sequence was more complex.

Cell Testing
Tables 2, 3 and 4 summarize the I-V data for the various runs.

For these tables, we used the I-V data for the best cell of the four cells obtained from the starting substrates. We have also applied an AR coating gain of 33% to Isc (and to efficiency).

We note that in Table 2, the GaInAs samples grown on GaAs substrates had significantly better performance than samples grown on Ge substrates. Our decision to complete all the runs in close sequence did not allow the possibility of optimizing the GaAs seeding layer on the Ge, or even in optimizing the various layer growths on GaAs substrates. When we plotted the trend in the I-V parameters in Table 2 versus lattice-mismatch, we found that Voc (and CFF) decreased steadily as expected, but that Jsc also decreased, not as expected. These

reduced Jsc values indicated either substrate and seeding layer deficiencies, and/or ineffective lattice grading layers. The Jsc decrease showed that practical losses offset the theoretical increase at the lower bandgaps. The tandem structures also give significantly lower CFF (and Voc) values than the single cell structures, indicating that the lattice-mismatch was more severe for the more complex structures, especially when GaInP layers were used.

In a later section we will give some conclusions on the cell I-V data, and also on the characterization methods tried.

Characterization

X-Ray Diffraction
We used double crystal X-ray diffraction to attempt to evaluate the degree of strain and of lattice-mismatch. Some of our X-ray results on the GaInAs cells are shown in Figures 6 through 10.

Figure 6 shows the diffraction pattern for sample #6-3464 ($Ga_{0.95}In_{0.05}As$ layers grown on a GaAs substrate) The GaAs peak is very narrow, showing little strain. The GaInAs peak is probably that shown at -400 arc-sec and its width indicates some residual strain. Using Vegard's Law for y = 0.935, the mismatch is around +0.47% and the peak at -400 arc-sec suggests that RTI has obtained some lattice-grading. The weak X-ray peak at +1488 arc-sec could indicate a growth anomaly, such as variable Ga/In ratios or superlattices in the grown layers.

Figures 7 through 10 are diffraction figures for GaInAs samples grown on Ge substrates, with a thin seeding layer of GaAs. Figures 7, 8, 9 and 10 show the plots obtained for 10%, 15%, 20% and 25% In content. Because the Ge substrates are deliberately misoriented from the (100) orientation, the tests often show different results for plots made at +8° and -8° from the horizontal orientation. In principle the In (or Ga) content can be estimated from the average of these 2 plots; however we observe it is not always clear which peak shows the layer with the required composition. In some cases, extra peaks, possibly caused by the grading layers are observed.

We also had one sample (6-3776, with 25% In content) characterized outside with triple crystal X-ray diffraction. The triple crystal instrument could provide both diffraction space maps as well as rocking curves, without the need for alignment to change the optics.

Figure 11 shows a slice taken through a diffraction space map. Figure 12 shows the same plot overlaid with a simulation plot for $Ga_xIn_{1-x}As$ layers where x varies from 0.95 to 0.75. The measured peak is close to x = 0.88 (1-x = 0.12) but the individual layers do not show clearly.

We concluded that although X-ray data could provide some insight, we could not obtain quantitative resolution of the various layers. We do not plan extensive X-ray evaluation of the later growth sets.

Quantum Efficiency (QE)
We use QE measurements to show the spectral response of the cells, and also to determine the bandgap from the response near the cut-off wavelength. We are completing these bandgap measurements for all three sets of cells.

Other Characterization Methods
Microscopic examination of the surface layers did not show systematic increase in growth-generated surface defects. We are also defining etchants to use to show the dislocation density in the grown layers over the composition range of the structures.

CONCLUSIONS

Overall we conclude that growth on Ge substrates, possibly because of the GaAs seeding layer obtained in a single growth, gives lower cell performance than growth on GaAs substrates.

The target compositions (x or y values) were not always obtained (the measured bandgaps differed from the target values).

Also there are indications that the lattice grading layers did not reduce strain sufficiently, particularly for the GaInP layers or for the tandem cell structures which are relatively complex.

As mentioned above, this indicates that our rapid scan approach was not as successful as a systematic iterative program.

We can conclude from this scan, that it is essential to optimize the substrate quality and to systematically refine the lattice-grading procedures, in order to determine if the deleterious lattice-mismatch effects can be reduced to allow the optimum bandgap pairs to give higher efficiency.

Our X-ray results also showed that in addition to dislocation counts, we need other characterization methods to assess the lattice-strain. At present the detailed trend of the I-V parameters is the best indicator, and we are investigating a wide range of the cell properties (especially dark diode characteristics) to use as indicators.

We are completing characterization of cells in all three growth sets.

REFERENCES

1) J.C.C. Fan, B-S Tsaur and B.J. Palm "Conference Proceedings of the 16th IEEE PVSC, 1983, P. 692
2) M. Wanlass "Photonics Spectra" November 1992, P. 159

Table 1

Estimates for AM0 Efficiency for Several Bandgap Pairs

Pair	E_g values (eV)	x in $Ga_xIn_{1-x}P$	y in $Ga_yIn_{1-y}As$	Theoretical AM0 Eff (%)	Lattice Mismatch to Ge (%)	Lattice Mismatch to GaAs (%)
A	1.9 1.42	.53	1.0	28.6	0	~0
B	1.89 1.37	.52	.95	29.2	+0.35	+0.36
C	1.865 1.32	.50	.90	29.8	+0.70	+0.72
D	1.825 1.265	.47	.85	30.2	+1.05	+1.076
E	1.80 1.21	.455	.80	30.8	+1.40	+1.44
F	1.77 1.16	.43	.75	31.0	+1.75	+1.80
G	1.73 1.11	.40	.705	31.6	+2.09	+2.12
H	1.70 1.06	.375	.65	31.7	+2.47	+2.51
I	1.65 1.02	.34	.62	31.1	+2.69	+2.725
J	1.35 0.75	0	.47	24	+3.75	+3.8

Table 2
I-V Data For Ga$_x$In$_{1-x}$As Cells

RTI Growth #	Structure	Target Values			Measured Values			
		In Content (1-x)	Eg (eV)	Eff (%)	Voc (mV)	Jsc (mA/cm²)	CFF (%)	Eff (%)
-	Control GaAs/Ge	0	1.42	18.8	1020	32	78	18.8
6-3464	GaInAs/GaAs	0.05	1.37	18.6	938	34.1	77.7	18.4
6-3741	GaInAs/Ge	0.05	1.37	18.6	790	16.5	74.8	9.2
6-3742	GaInAs/Ge	0.05	1.37	18.6	903	17.8	79.2	9.4
6-3747	GaInAs/Ge	0.10	1.32	18.3	830	16.5	75.9	7.7
6-3751	GaInAs/Ge	0.15	1.265	17.8	813	12.2	70.1	5.2
6-3773	GaInAs/Ge	0.20	1.21	17.3	514	12.4	69.6	3.2

Table 3
I-V Data for Ga$_y$In$_{1-y}$P Cells (on Ga$_z$In$_{1-z}$As Layers)

RTI Growth #	Structure	Target Values				Measured Values			
		(1-y)	(1-z)	Eg (eV)	Eff (%)	Voc (mV)	Jsc (mA/cm²)	CFF (%)	Eff (%)
6-4028	GaInP on GaInAs Grading layers	0.48	0.05	1.89	18.15	1077	13.0	73.5	7.7
6-4039		0.50	0.10	1.865	18.35	816	14.35	75.4	6.65
6-4040		0.53	0.15	1.825	18.5	799	14.63	6.9	6.0
6-4029		0.545	0.20	1.80	18.7	879	14.9	62.1	6.0
6-4042		0.57	0.25	1.77	18.9	786	16.0	75	6.9

Table 4
I-V Data for Ga$_y$In$_{1-y}$P on Ga$_x$In$_{1-x}$As Cells (on Ge Substrates)

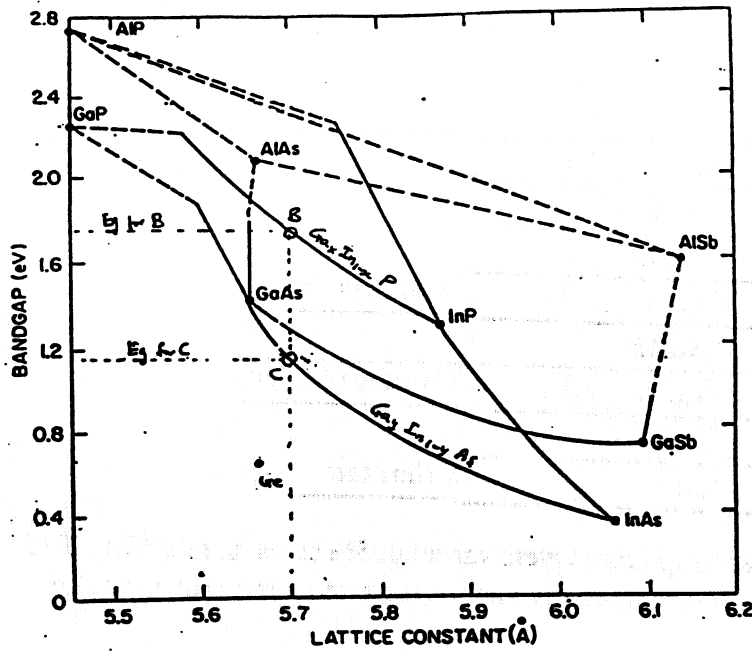| RTI Growth #	Structure	Target Values				Measured Values			
		(1-y)	(1-x)	Eg (eV)	Eff (%)	Voc (mV)	Jsc (mA/cm²)	CFF (%)	Eff (%)
6-4040	GaInP/GaInAs tandem cells on GaInAs grading layers	0.48		1.89	26.0	1634	12.75	55.7	8.5
			0.05	1.37					
6-4045		0.50		1.865	26.5	1718	13.4	54.3	9.2
			0.10	1.32					
6-4044		0.53		1.825	26.9	890 (as high as 1205)	14.35	49.6	4.7
			0.15	1.265					

Figure 1
Bandgap versus Lattice Constant (III-V Alloys)

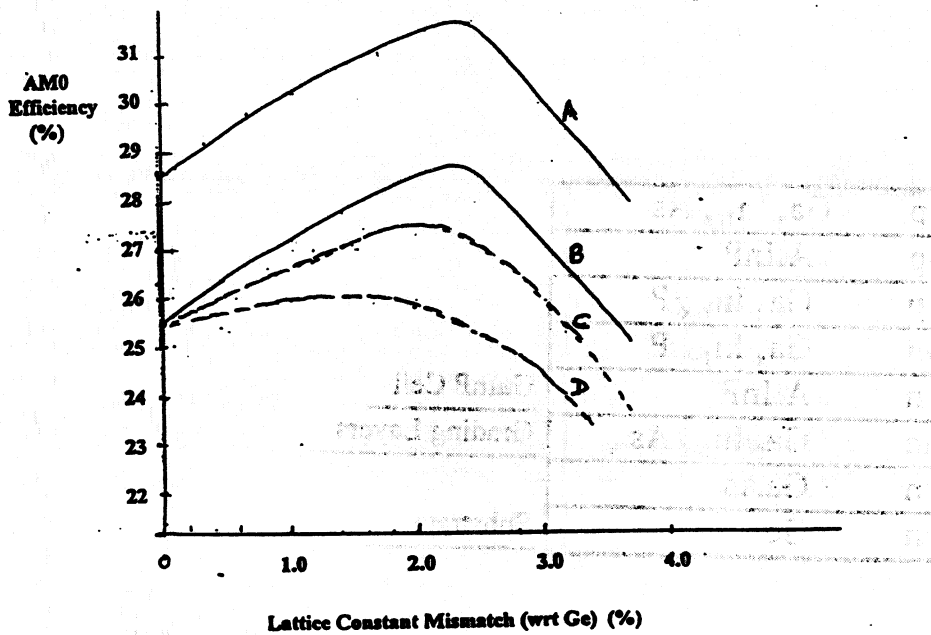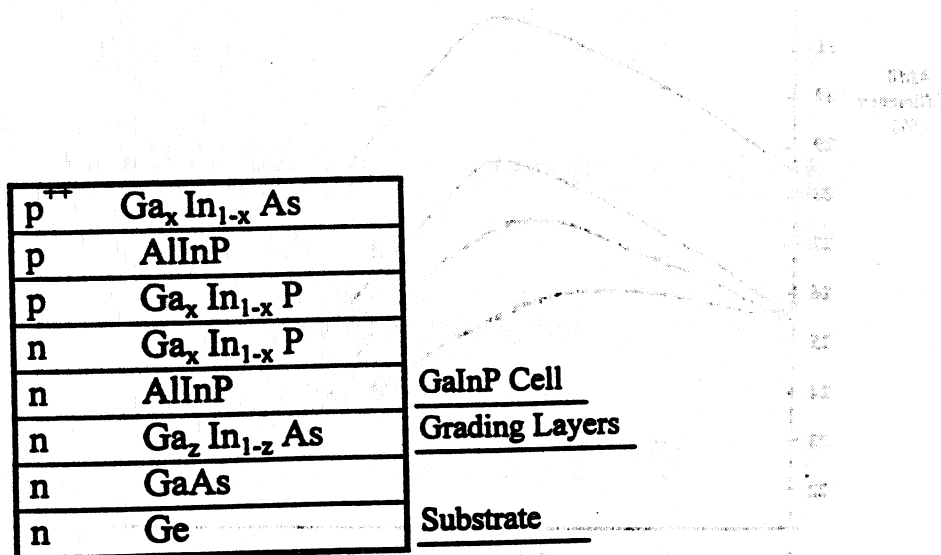The GaInP and GaInAs tie-lines are shown. B and C are typical bandgap pairs.

Figure 2

AM0 Efficiency versus Lattice Constant Mismatch
(For Selected Bandgap Pairs)

p^{++}	$Ga_y In_{1-y} As$	
p	GaInP	
p	$Ga_y In_{1-y} As$	
n	$Ga_y In_{1-y} As$	GaIn As Cell
n	GaInP	
n	$Ga_z In_{1-z} As$	Grading Layers
n	GaAs	
n	Ge	Substrate

z values in grading layers varied in 5% steps from 0.95 to 0.75
y values selected to give lattice match to appropriate z-value

Figure 3 Layer Sequence for $Ga_y In_{1-y} As$ Cells

p^{++}	$Ga_x In_{1-x} As$	
p	AlInP	
p	$Ga_x In_{1-x} P$	
n	$Ga_x In_{1-x} P$	
n	AlInP	GaInP Cell
n	$Ga_z In_{1-z} As$	Grading Layers
n	GaAs	
n	Ge	Substrate

z values in grading layers varied in 5% steps from 0.95 to 0.75
x values selected to give lattice match to appropriate z-value

Figure 4 Layer Sequence for $Ga_x In_{1-x} P$ Cells

p^{++}	$Ga_y In_{1-y} As$	
p	AlInP	
p^+	$Ga_x In_{1-x} P$	
n	$Ga_x In_{1-x} P$	
n	AlInP	GaInP Cell
n^{++}	$Ga_y In_{1-y} As$	
p^{++}	$Ga_y In_{1-y} As$	Tunnel Junction
p^+	GaInP	
p^+	$Ga_y In_{1-y} As$	
n	$Ga_y In_{1-y} As$	
n	GaInP	GaInAs Cell
n	$Ga_z In_{1-z} As$	Grading Layers
n	GaAs	
n	Ge	Substrate

x- and y-values selected to give lattice-match to appropriate z-values

Figure 5 Layer Sequence for Tandem Cell
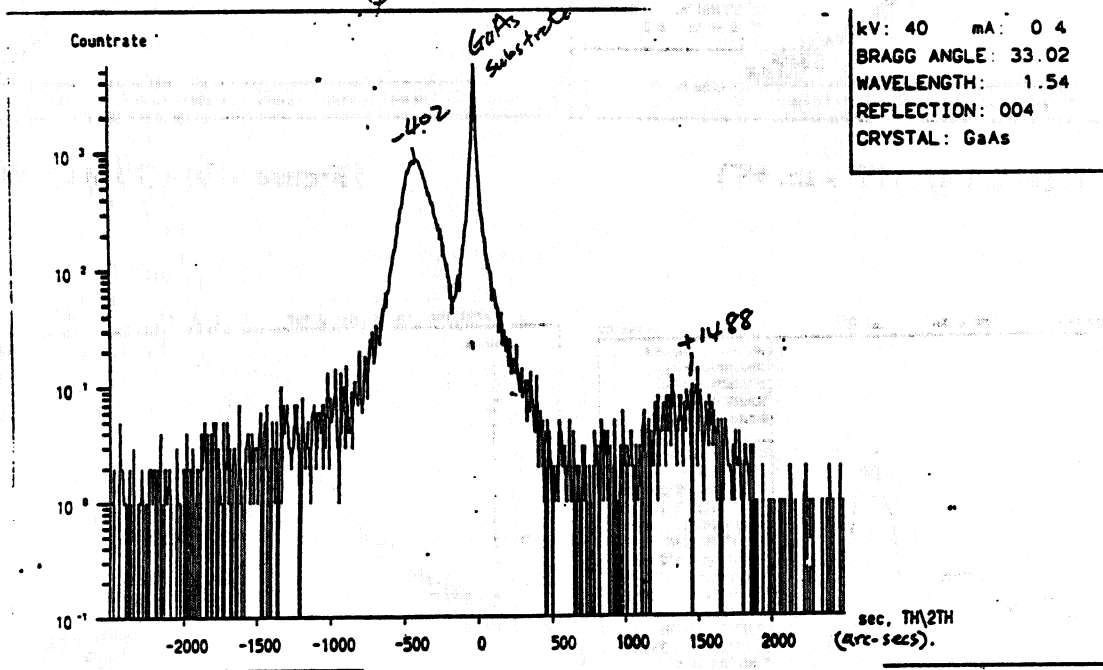
Figure 6

X-Ray Diffraction for RTI #6-3464
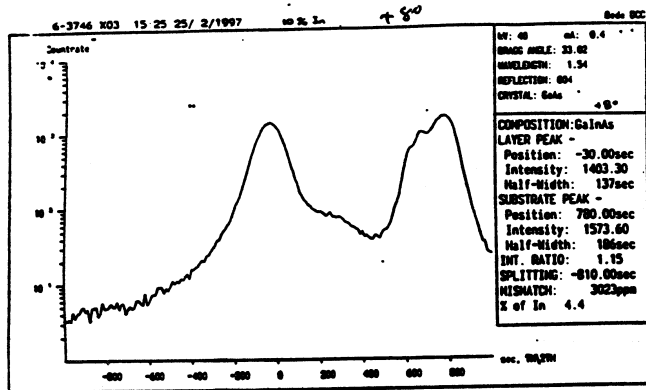
Figure 7 (10% In, +8°)
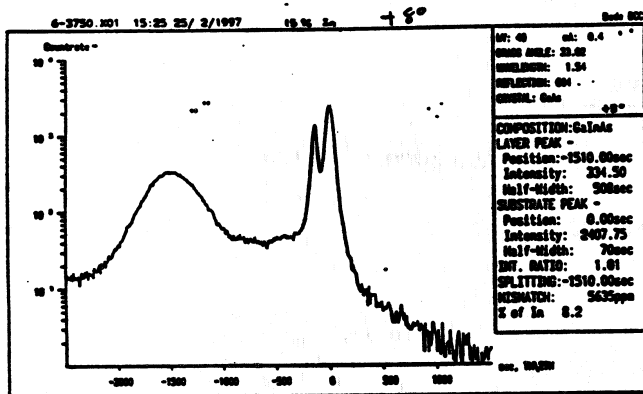
Figure 8 a) - (15% In, +8°)
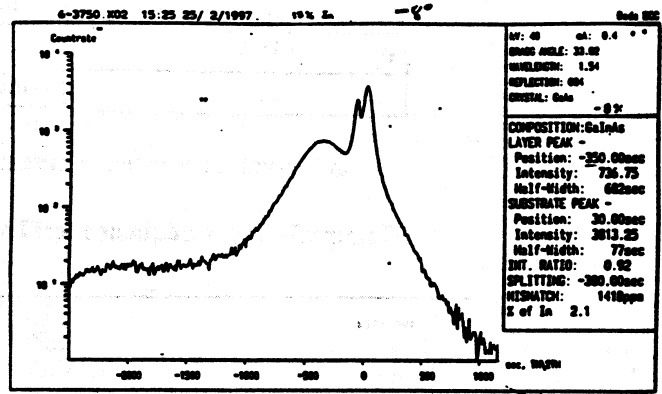
Figure 8 b) - (15% In, -8°)
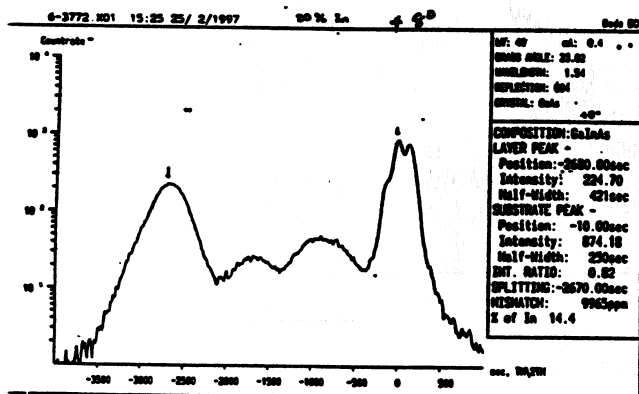
Figure 9 (a) - (20% In, +8°)
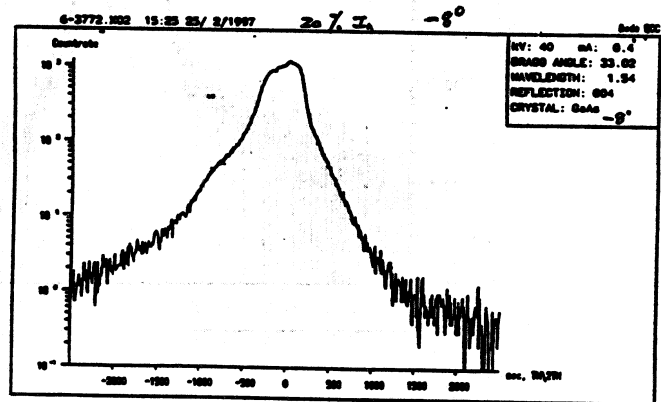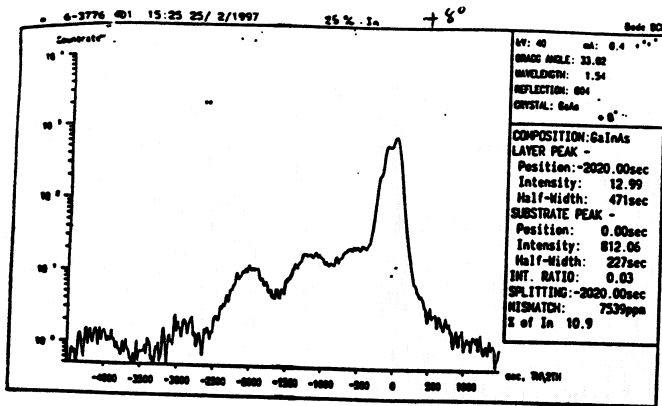

Figure 9 b) - (20% In, -8°)
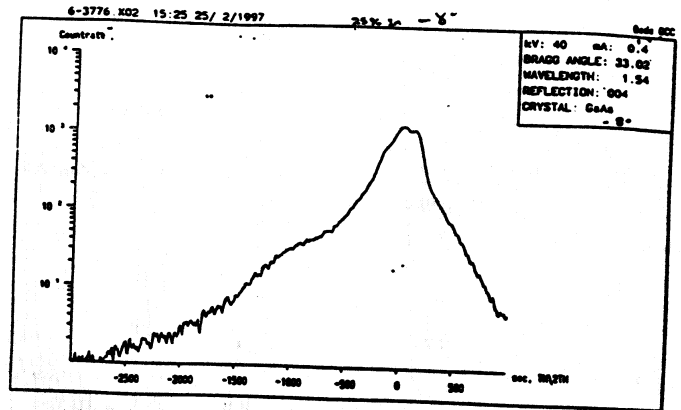
Figure 10 a) - (25% In, +8°)
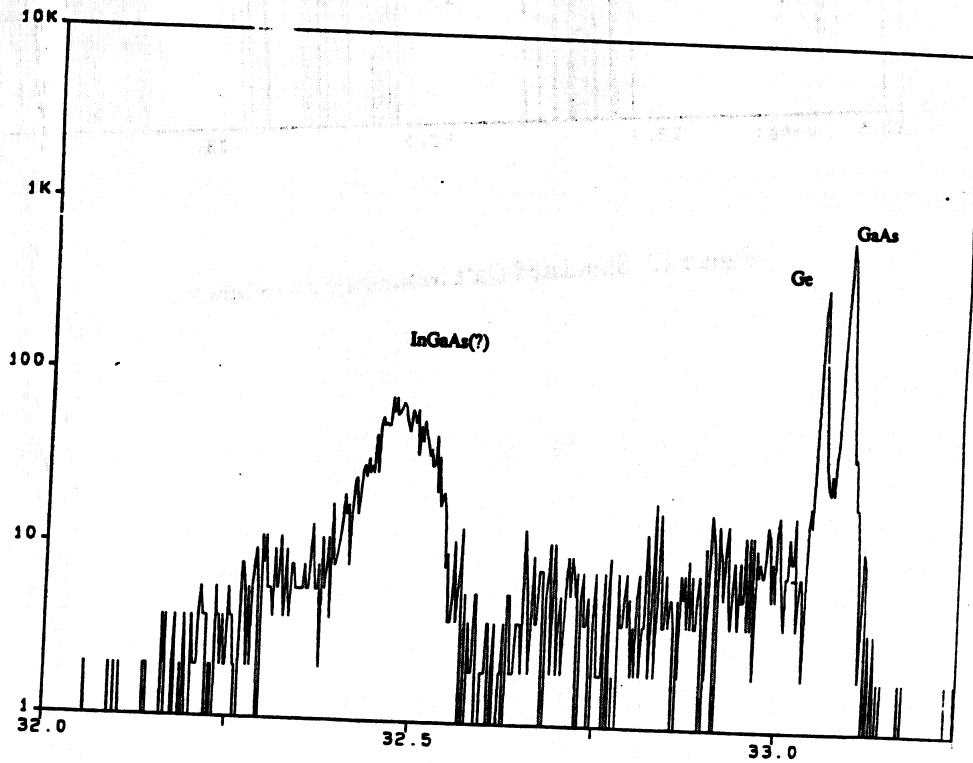

Figure 10 b) - (25% In, -8°)

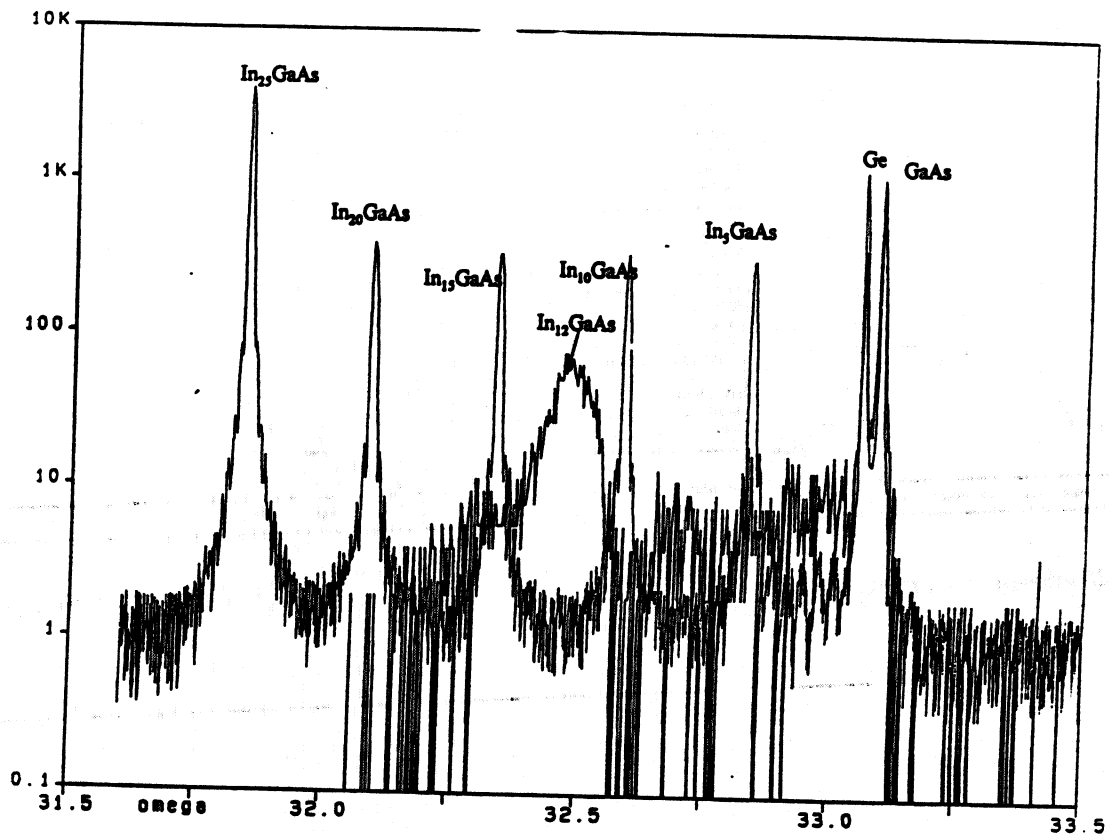

Figure 11 Section of Diffraction Space Map through the Substrate Maximum

Figure 12 Simulated Data Modeled In% as Shown